Electrosynthesis and redox behavior of vinylogous TTF displaying strong conformational changes associated with electron transfers

ARTICLE *in* ELECTROCHIMICA ACTA · JULY 2001

Impact Factor: 4.5 · DOI: 10.1016/S0013-4686(01)00619-3

5 AUTHORS, INCLUDING:

Dominique Lorcy
Université de Rennes 1

124 PUBLICATIONS **1,617** CITATIONS

SEE PROFILE

PERGAMON

Electrochimica Acta 46 (2001) 3269–3277

ELECTROCHIMICA Acta

www.elsevier.com/locate/electacta

Electrosynthesis and redox behavior of vinylogous TTF displaying strong conformational changes associated with electron transfers

R. Carlier [a], P. Hapiot [b,*], D. Lorcy [a,1], A. Robert [a], A. Tallec [a]

[a] *Synthèse et Electrosynthèse Organiques, UMR CNRS 6510, Université de Rennes 1, campus de Beaulieu, 35042 Rennes Cedex, France*

[b] *Laboratoire d'Electrochimie Moléculaire de l'Université Denis Diderot-Paris 7, UMR CNRS N°7591, 2 place Jussieu, Case courier 7107, 75251 Paris Cedex 05, France*

Received 17 November 2000; received in revised form 28 February 2001

Abstract

The redox properties of a series of substituted vinylogous tertrathiafulvalenes (TTF) prepared by oxidative coupling of 1,4-dithiafulvenes (DTF) have been investigated in acetonitrile and dichloromethane. The different steps of the electrodimerization mechanism have been characterized: fast electron transfer, coupling between two cation-radicals and slow deprotonation. Through the substituent choice of DTF, it is possible to control the relative stabilities of the different redox species of the electrogenerated vinylogous TTF. According to the nature and position of the substituent, the structural changes induced by the steric interactions lead to a compression of potential (where the second electron is easier to remove than the first one), or on the contrary to a large increase of the separation between the first and second oxidation potentials (by comparison with similar molecules without steric hindrance). Density functional modeling calculations and detailed analysis of the electrochemical behavior have been used to rationalize the substituent effect. A good agreement with the occurrence of an EE mechanism in which the electron transfer is concerted with the conformation changes is found. The inner reorganization energies are low (0.35–0.45 eV) allowing a fast passage between the different conformations during the electron transfers.

Keywords: Electrosynthesis; Redox behavior; Vinylogous TTF

1. Introduction

Tetrathiafulvalenes (TTF) and their analogues are the subject of intense researches in an attempt to prepare novel organic materials (for general reviews see Refs. [1–7]). In this connection, the preparation of substituted vinylogous TTF **4** by oxidative coupling of 1,4-dithiafulvenes (DTF) (**3**) has attracted a lot of attention due to the ability of the method for introducing different types of substituent on the central conjugation [8–21]. A detailed mechanistic analysis of the electrodimerization reaction was first performed [12] allowing a better knowledge of the global reaction. Following this strategy, we prepared various TTF vinylogues **4** with phenyl groups (R) substituted on their *para*- or *ortho*-positions by different donating or withdrawing substituents. The choice of these substituents

* Corresponding author. Tel.: +33-2-9928-5939; fax: +33-2-9928-6738.

E-mail address: philippe.hapiot@univ-rennes1.fr (P. Hapiot).

[1] Also corresponding author.

0013-4686/01/$ - see front matter
PII: S0013-4686(01)00619-3

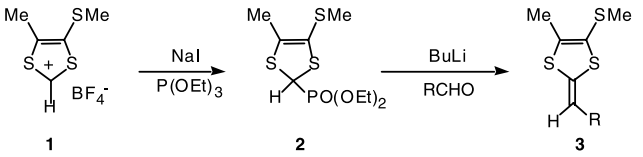

Scheme 1.

was made in order to modify both the steric hindrance and the electronic properties.

The electrochemical behavior of the produced dimer strongly depends on the nature and position of the substituent on the phenyl ring. For some of these compounds, a reversible bielectronic transfer leading directly to the dicationic state was observed by cyclic voltammetry [22]. This result was in contrast with that of similar TTF vinylogues with one vinyl spacer, for which two monoelectronic transfers are generally observed [1–7]. In preliminary studies, we have observed large conformational modifications between the neutral and the dicationic states. The addition of bulky substituents on the central conjugation prevents the molecule to be planar due to the steric interactions [11–18]. By analogy with literature results concerning the 'inverted potentials', i.e. redox systems where the second electron is easier to remove than the first one [23–29], we suggest that the conformational modifications induced by the steric interactions were responsible for the unusual redox behavior observed for these TTF. However, several questions remain especially concerning the variation of the relative order of the potentials in a same family or the timing for the different steps (electron transfer, conformational changes, etc.). Indeed, situations of 'normal order of potentials' or on the contrary of 'inverted potentials' are observed for molecules with similar steric constraints. Thus, to be able control the modifications of conformation occurring during the electron transfer and to rationalize the effect, we investigated the redox properties and compared the experimental results with molecular modeling and X-ray structure determinations.

2. Experimental

2.1. Chemical synthesis of dithiafulvenes 3

The starting materials, DTF **3** were prepared according to the chemical pathway described in Scheme 1. Dithiolylium tetrafluoroborate (**1**) reacted with triethylphosphite in the presence of sodium iodide to give the corresponding phosphonate **2** in quantitative yield. The synthesis of several DTF **3** was performed by a Wittig Horner type reaction [30] between (1-3-dithiole) phosphonate in basic medium and different aldehydes [11].

2.2. Macroscale electrolyses of vinylogous TTF 4

Preparative electrolysis was performed in a divided cell, the working electrode was a platinum grid. In a typical experiment, 50 ml of an acetonitrile solution containing 2×10^{-3} mol l^{-1} of the DTF **3** and 1 mol l^{-1} of tetrabutylammonium hexafluorophosphate is introduced in the working compartment. The solution is then oxidized under controlled potential (0.6–0.8 V vs. aqueous SCE, depending on R). Coulometric measurements show that 2 mol of electron per mol of substrate is required for complete oxidation. The highly colored solution is then, without any treatment, reduced at -0.2 V/SCE. Complete reduction is achieved after consumption of 1 mol of electron per mol of substrate. Work up of the solution leads to neutral dimer **4** in good yields (Scheme 2).

We also prepared the unsubstituted derivatives **5**, as outlined in Scheme 3, in order to compare the electrochemical behavior of derivatives **4** with this reference compound **5** [2].

2.3. Cyclic voltammetry

All the cyclic voltammetry experiments were carried out at 20 ± 0.1 °C using a cell equipped with a jacket allowing a circulation of water from the thermostat. The counter electrode was a Pt wire and the reference electrode an aqueous saturated calomel electrode ($E°$/SCE = $E°$/NHE − 0.2412 V) with a salt bridge containing the supporting electrode. The SCE electrode was standardized against the ferrocene/ferricinium couple, $E° = +0.405$ V/SCE in acetonitrile and $+0.528$ V/SCE in CH_2Cl_2.

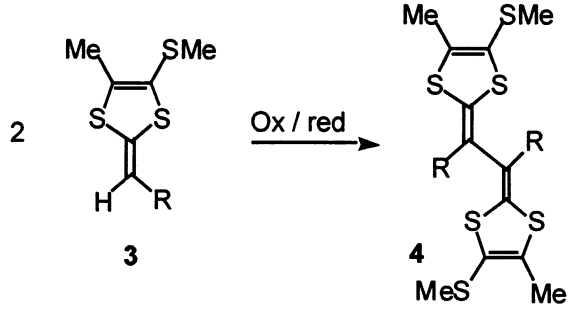

Scheme 2.

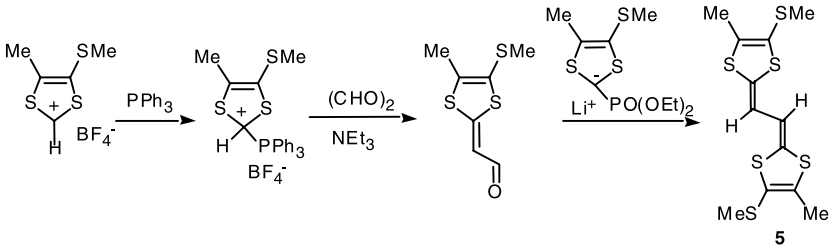

Scheme 3.

For low scan rate cyclic voltammetry (0.05–500 $V\,s^{-1}$), the working electrode was either a glassy carbon disk (0.8 mm diameter Tokai Corporation), a 1 mm diameter gold or platinum disk. They were carefully polished before each set of voltammograms with 1 μm diamond paste and ultrasonically rinsed in absolute ethanol. Electrochemical instrumentation consisted of a PAR Model 175 Universal programmer and of a home-built potentiostat equipped with a positive feedback compensation device [31]. The data were acquired with a 310 Nicolet oscilloscope.

For high scan rate cyclic voltammetry, the ultramicroelectrode was a gold or platinum wire (10 μm diameter) sealed in soft glass [32]. The signal generator was a Hewlett–Packard 3314A and the curves were recorded with a 4094 C Nicolet oscilloscope with a minimum acquisition time of 5 ns per point.

Acetonitrile was of Uvasol quality (Merck) and was used as received. The supporting electrolyte NEt_4BF_4 and 2,6-lutidine (2,6-dimethylpyridine) were from Fluka (puriss).

Simulations of the voltammograms were made with the BAS Digisim® simulator 2.1 [33]. Molecular modeling were performed using the GAUSSIAN 98 [34] package for density functional and solvation calculations.

3. Results and discussion

All the investigated DTF exhibit the same general redox behavior. On the first anodic scan, DTF **3** displays an irreversible oxidation peak (see example DTF **3b**, Fig. 1a). A new reversible system is observed at a less positive potential during the following scans. The first electrochemical oxidation (peak II), corresponding to the oxidation of DTF **3** to its cation radical $\mathbf{3}^{\bullet+}$, is followed by a series of chemical reactions leading to **4**, which is further oxidized at less positive potentials. The new redox (I) system is associated with the redox behavior of dimer **4** formed in the solution. It is interesting to notice that the peak (I) is less than half of the oxidation peak (II) showing that a low quantity of dimer **4** was formed during the scan.

3.1. Mechanism of dimer formation

The electrodimerization reaction involves different electrochemical and chemical steps: homogeneous and heterogeneous electron transfers, carbon–carbon bond formation and elimination of protons. The first oxidation step of **3** leads to the formation of the cation-radical that can be observed through the reversibility of its voltammogram (for scan rates higher than 5000–10 000 $V\,s^{-1}$, see Fig. 1b). Addition of large amounts of base (2,6-lutidine) to the solution does not change the reversibility of the fast scan voltammogram indicating that the lifetime of the cation-radical is not modified. At the lowest scan rates, an increase of the current of the reversible system corresponding to the quantity of produced dimmer is noticed. From these observations, we can conclude that the first reaction step is not a

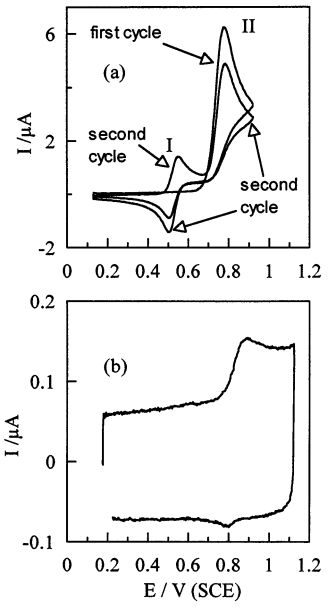

Fig. 1. Cyclic voltammetry of a solution of 10^{-3} mol l^{-1} of DTF **3b** ($R = p\text{-}NCC_6H_4$) in acetonitrile ($+0.2$ mol l^{-1} of NEt4BF4): (a) on a 1 mm diameter platinum disk electrode, scan rate = 0.2 $V\,s^{-1}$; (b) on 10 μm diameter microelectrode, scan rate = 6000 $V\,s^{-1}$.

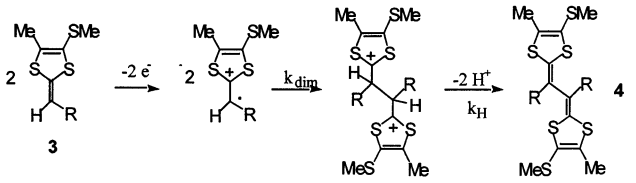

Scheme 4.

deprotonation and thus that this step occurs after the carbon–carbon bond formation.

The next problem concerns the nature of the coupling step. Does it involve the reaction between the two electrogenerated cation-radicals or the addition of the cation-radical with the starting molecule [35,36]? In a series of voltammetry experiments, we studied the variations of the peak potential as a function of the experimental parameters as the theoretical variations are different for the two mechanisms. For example for **3b**, we found that the anodic peak potential varies linearly with the logarithm of the scan rate with a slope, $\partial E_p/\partial(\log(v)) = 19.9$ mV, and with the bulk concentration of the DTF $\partial E_p/\partial(\log(c) = -19.4$ mV per 10-fold increase. Similar slopes and behaviors were found for all the studied compounds. These observations agree with a fast electron transfer to form a cation radical $\mathbf{3}^{\bullet+}$, followed by the irreversible coupling of two cation radicals leading to the protonated dimer [12]. Then, this protonated dication deprotonates into the expected TTF vinylogue **4** (see Scheme 4).

After having determined the nature of the reaction mechanism, kinetic and thermodynamic constants were measured by analysis of the experimental voltammograms measured at high scan rates. The dimerization rate constants, k_{dim}, were determined by comparison with simulated curves. The values of k_{dim} do not change significantly with the nature of the substituents ranging from 2×10^8 to 4×10^8 l mol^{-1} s^{-1} (see Table 1). The low formation of **4** is thus related to kinetic limitations during the deprotonation leading to the dimer and the deprotonation step occurs a long time after the carbon–carbon bond formation. This result was confirmed by the low deprotonation kinetic constants in acetonitrile (without added base), k_H in the range 0.2–1.0 s^{-1}. After having established the sequence of the different reaction steps leading to the formation of TTF vinylogues **4**, we focused on the electrochemical behavior of these derivatives.

3.2. Redox behavior of substituted vinylogous TTF *4*

Investigations of the vinylogous TTF **4** and **5** were performed in acetonitrile and in dichloromethane (see Fig. 2). Depending on the substituent and on the solvent, two single-electron reversible transfers or one two-electron reversible process were observed. For the oxidation of TTF containing the aromatic groups with *para*-substituent (**4a**–**g**), cyclic voltammetry experiments display only one bielectronic process in acetonitrile. In the investigated range of scan rates (0.05–5000 V s^{-1}), no other intermediate was observed. As calculated before [37,38], assuming that both electron transfers are fast, the potential peak separation $\Delta E_p = E_{pa} - E_{pc}$ allows a direct measurement of the difference in standard (formal) potentials $\Delta E° = E°_2 - E°_1$. For an infinite separation, ΔE_p tends to 28.25 mV at 20 °C, meaning that the measurement of the individual potentials becomes very inaccurate (then impossible) for large inversions of potential. In fact, the kinetics of the electron transfers has the effect of increasing ΔE_p resulting as an overestimation of $\Delta E°$. Taking into account these limitations, data from Table 2 show the clear inversion of the individual reversible

Table 1
Thermodynamic and kinetics parameters for the oxidation of DFT **3**

Compounds	R	$E°_{DTF}$ (V)	k_{dim} (l mol^{-1} s^{-1})	k_H (s^{-1})
3a	*p*-$NO_2C_6H_4$	0.869	3×10^8	0.3
3b	*p*-NCC_6H_4	0.838	2×10^8	0.3
3c	*p*-ClC_6H_4	0.767	2×10^8	0.2
3d	*p*-C_6H_4	0.733	2×10^8	0.3
3e	*p*-MeC_6H_4	0.707	2×10^8	0.2
3f	*p*-$MeOC_6H_4$	0.637	4×10^8	1.0
3g	*p*-$(Me)_2NC_6H_4$	0.406	5×10^5	–

Error on $E° \pm 10$ mV. Error on kinetics constants $\pm$ a factor of 2.

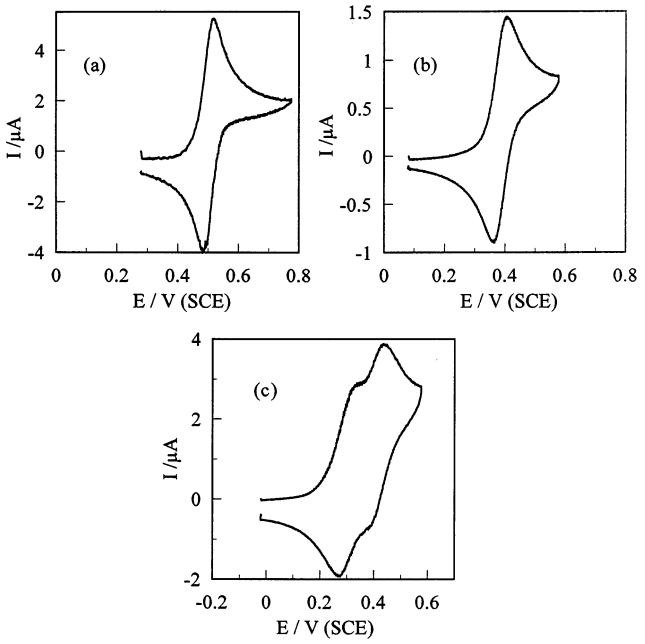

Fig. 2. Cyclic voltammetry of TTF vinylogues oxidation on a 1 mm Pt electrode in acetonitrile + 0.1 mol l^{-1} NEt_4BF_4. Scan rate: 0.2 V s^{-1}. Temperature = 20 °C: (a) **4b** (R = *p*-NCC_6H_4), concentration = 4.5×10^{-4} mol l^{-1}; (b) **4f** (R = *p*-$MeOC_6H_4$), concentration = 6×10^{-4} mol l^{-1}; (c) **5** (R = H), concentration = 8.5×10^{-4} mol l^{-1}.

formal potentials (the second electron being more easily removed than the first one). The second noticeable observation is that the inversion of the individual formal potentials is larger when a withdrawing group is present on the phenyl ring. Similar trends were found from the investigations performed in dichloromethane. The use of this solvent instead of acetonitrile induced an increase of $\Delta E°$ for all the investigated vinylogous TTF as expected from the lower dielectric constant of dichloromethane. In CH_2Cl_2, depending on the donat-

Table 2
Oxidation potentials of TTF vinylogues **4** and **5** assuming fast electron transfers

	R	CH_3CN		CH_2Cl_2	
		$E°_{2e-}$ (V)(ΔE_p in mV)[a]	$\Delta E° = E°_2 - E°_1$ (V)	$E°_{2e-}$ (V) (ΔE_p in mV)[a]	$\Delta E° = E°_2 - E°_1$ (V)
4a	*p*-$NO_2C_6H_4$	0.546 (31)	−0.065	0.671 (34)	−30
4b	*p*-NCC_6H_4	0.530 (30)	−0.090	0.651 (35)	−25
4d	C_6H_5	0.413 (37)	−0.013	0.519 (104)[b]	76
4f	*p*-$MeOC_6H_4$	0.378 (41)	0.004	0.468 (143)[b]	104
4g	*p*-$Me_2NC_6H_4$	0.309 (41)	0.004	0.334 (60)[c] 0.454 (61)	120
4h	*o*-$NO_2C_6H_4$	0.467 (92)[b]	0.067	0.495 (57)[c] 0.716 (63)	221
4i	*o*-NCC_6H_4	0.519 (109)[b]	0.079	0.551 (57)[c] 0.767 (70)	216
4j	*o*-$MeOC_6H_4$	290 (56)[c] 402 (59)	0.112	0.293 (59)[c] 0.551 (63)	258
5	H	0.321 (57)[c] 0.436 (57)	0.142	0.398 (56)[c] 0.579 (57)	181

[a] ΔE_p at 0.1 V s^{-1}.
[b] Double wave.
[c] Two well-separated waves ($\Delta E_p = E_{pa2} - E_{pc1}$).

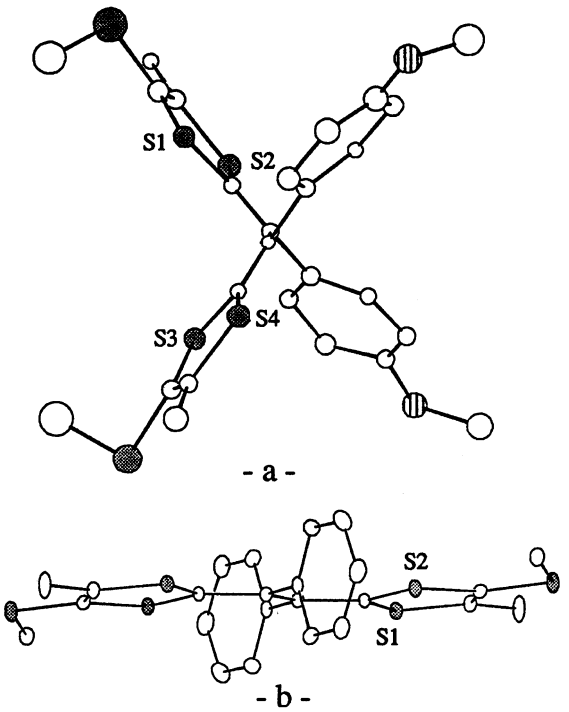

Fig. 3. X-ray investigations: (a) molecular structure of **4f** (from Ref. [11]); (b) molecular structure of the dicationic vinylogous TTF **4d** (from Ref. [40]), counteranion: I_3^-.

ing properties of the phenyl group the bielectronic waves can split or not into two monoelectronic ones, but the same general effect is observed for all the TTF in both solvents.

When a substituent is introduced on the *ortho*-position of the phenyl group (**4h**–**j**), similar decreases of $\Delta E°$ are observed as a function of the withdrawing strength of the substituent. However, the extracted $\Delta E°$ are always larger for the *ortho*-substituted molecules than for the corresponding *para*-substituted molecules.

These analyses were confirmed by spectrovoltammetry experiments [22]. The spectrum of the electrogenerated radical-cation was clearly visible before the formation of the dication in the case of the non-substituted derivative **5** and in the case of electron donating substituents linked to **4**. On the contrary, the dication is directly produced during the oxidation in the case of withdrawing substituents.

3.3. X-ray structural investigations

The single-crystal X-ray analysis of a neutral donor **4f** reveals a non-planar geometry due to steric hindrance [11]. This severely distorted structure [22,39,40] was found for all the substituted TTF vinylogues [16–18]. After a chemical oxidation either with a solution of $Cu(ClO_4)_2 \cdot 6H_2O$ in THF or by exposing a solution of a donor in CH_2Cl_2 to an iodine atmosphere, the X-ray structures of several of these donors were determined [22,39,40]. The donor under its cation radical or dicationic forms adopts a new conformation with a planar extended TTF core while the substituents are located in a perpendicular plane (Fig. 3). Yamashita et al. observed similar conformational modifications on cation radical salts of vinylogous TTF substituted by bulky groups [17]. Interestingly, neutral non-substituted derivatives (R = H), analogues of **5**, are planar and do not undergo conformational changes upon oxidation as the extended TTF core remains planar.

3.4. Molecular modeling

The crystallographic data support the hypothesis that the unusual redox behavior for the TTF vinylogues is caused by structural changes. More surprisingly is the way that the oxidation potentials separations $\Delta E°$ vary with the substitution. To rationalize the effects, we performed a series of molecular modeling calculations to determine both the geometries and the stabilities of the TTF vinylogues in their three oxidation states.

The geometries were determined by full optimizations of the conformations using the B3LYP density functional [41] and the 6-31G* basis set [42] (see Fig. 4). For **5**, the neutral, radical cation and dication were found to be planar in agreement with the X-ray structural investigations. For the phenyl-substituted donors **4**, the neutral are twisted and the radical cation and the dication display an almost planar TTF core. The situation changes when a donor group is introduced on the phenyl ring and the dication is not planar anymore. This change of behavior is explained by a better stabilization of the positive charges due to the conjugation with the phenyl ring bearing donor groups. It results in a competition between the stabilization energy brought by the conjugation at the level of the TTF core and the energy gained by the stabilization of the positive charge by the donor groups. In the case of the simple phenyl and, of course, for withdrawing substituents, the dication has a better advantage to make the TTF core planar. It is noticeable that the electronic effects due to the repulsion of the two positive charges are lowered in the presence of the solvent. Therefore, it is likely that the gas phase calculations overestimate the twisting of the TTF core in the charged states.

To discuss the variations of the oxidation potentials more precisely, we should estimate the solvation free energies because much of $\Delta G°_{disp}$ in gas phase has an electrostatic origin. We used the IPCM [43] method where the solvent is described as a dielectric continuum with the geometries previously optimized in gas phase.

$$2TTF^{\bullet +} \rightleftarrows TTF^{2+} + TTF, \quad \Delta G°_{disp}$$

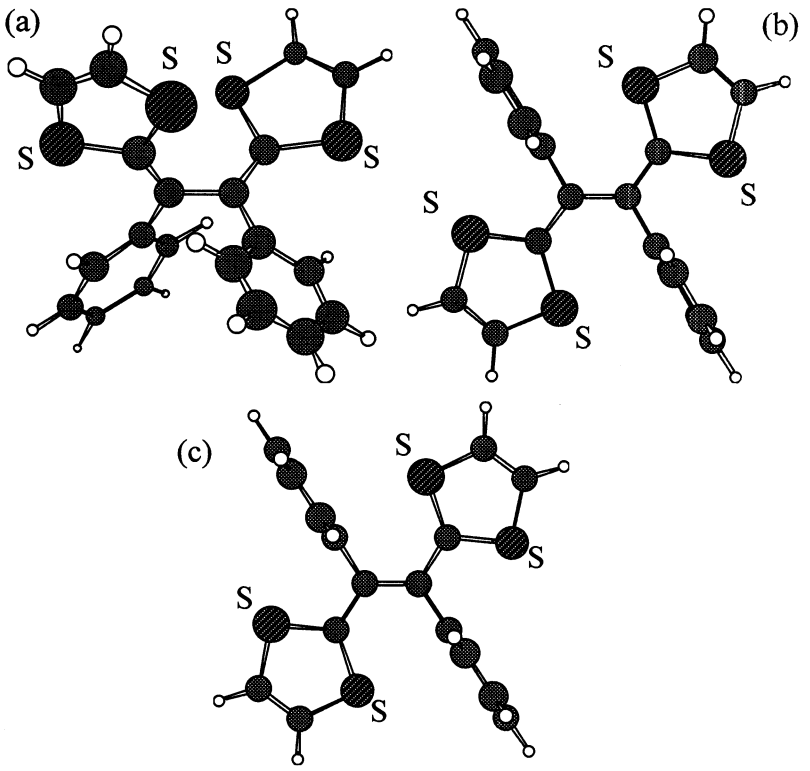

Fig. 4. Optimized geometries calculated at the B3LYP/6-31G* level, of the (a) neutral; (b) radical cation; (c) dication of **4d** ($R = C_6H_5$).

$\Delta G°$ in gas phase were estimated as the differences between the electronic energies [22]: $\Delta G°_{disp} \approx \Delta U_{el}(\text{dication}) + \Delta U_{el}(\text{neutral}) - 2\Delta U_{el}(\text{radical cation})$ $\Delta G°_{solv}(\text{dication}) + \Delta G°_{solv}(\text{neutral}) - 2\Delta G°_{solv}(\text{radical cation})$. The estimated absolute values were higher than the experimentally observed ones. If this overestimation is mainly due to the simplifications in the modeling, other factors like the ion pairing with the anion of the supporting electrolyte should also contribute to a decrease of $\Delta G°_{disp}$ [36]. The calculated $\Delta G°_{disp}$ values decrease when passing from the dichloromethane to the acetonitrile as we can expect from a lower repulsion energy between the positive charges in a solvent with a higher dielectric constant. The largest value is observed for the unsubstituted TTF vinylogue **5**, which displays experimentally the highest separation between the oxidation potentials. In the series of the phenyl-substituted compounds, the lowest $\Delta G°_{disp}$ value is obtained for **4b** ($R = p\text{-}NCC_6H_4$) and the highest for **4f** ($R = p\text{-}MeOC_6H_4$) in agreement with the experimental results.

Concerning the effect of the substituent position, a large increase of $\Delta G°_{disp}$ is calculated (0.13 eV) between **4b** and **4i**. To explain the additional influence of the *ortho*-position, we investigate the energies variations of each individual species ($\Delta U_{el} + \Delta G°_{solv}$) with the introduction of the steric hindrance. In acetonitrile, the derived differences $(\Delta U_{el} + \Delta G°_{solv})_{ortho} - (\Delta U_{el} + \Delta G°_{solv})_{para}$ for the CN substituted TTF **4b** and **4i** are 0.25, 0.16, 0.20 eV for the neutral, radical cation and dication, respectively. These differences confirm that the additional interactions between the *ortho* substituents and the TTF core result in higher destabilizations for the neutral and the dication species. The *ortho* effect canceled completely the compression of potentials in acetonitrile. In CH_2Cl_2, the $\Delta E°$ separation becomes even higher than for the unsubstituted TTF **5** (see Table 3). It results in a situation where the changes of conformation do not lead to compression as generally observed [23–29] but to an increase of $\Delta E°$.

Table 3
Estimated $\Delta G°_{disp}$ in eV using B3LYP/6-31G* in solvent

	R	CH_2Cl_2	CH_3CN
4b	$p\text{-}NCC_6H_4$	0.72	0.43
4d	C6H5	0.81	0.53
4f	$p\text{-}MeOC_6H_4$	0.88	0.61
4i	$o\text{-}NCC_6H_4$	0.85	0.56
5	H	1.06	0.75

Table 4
Experimental and theoretical kinetics parameters for the first electron transfer

	R	Experimental					Theoretical
		$\Delta E°$ (V)	$k_{s,1}$ (cm s^{-1})	λ_{e1ec} (eV)	$\lambda_{0,elec}$ (eV)	$\lambda_{i,e1ec}$ (eV)	λ_{elec} (eV)
4b	*p*-NCC_6H_4	−0.12	1–0.5	0.796–0.867	0.460	0.436	0.896
4f	*p*-$MeOC_6H_4$	0.004	2.0–1.5	0.726–0.755	0.453	0.347	0.800
5	H	0.142	4–3	0.679–0.708	0.536	0.163	0.699

3.5. Electron transfers kinetics

From the previous structural analysis, we have seen that most of the conformational changes occur after the first electron transfer. Thus, two limiting situations can be envisaged for the oxidation of **4**. In the first one, the changes of conformation are concerted with the first electron transfer resulting in a global EE mechanism.

$$TTF \rightleftarrows TTF^{\bullet +} + e^- \quad E_1^\circ, k_{s,1}$$

$$TTF^{\bullet +} \rightleftarrows TTF^{2+} + e^- \quad E_2^\circ, k_{s,2}$$

For previously described experiments where a concerted mechanism was suggested, the standard rates of heterogeneous electron transfers $k_{s,1}$ were reported to be slow [23–29] due to the large contribution to the activation barrier of the reorganization energy related to the structural changes. The second limiting situation is a stepwise mechanism (ECE type mechanism), a radical cation similar to the neutral species is produced, and then its conformation changes to give the more planar radical cation. In our systems, several observations were in favor of the concerted mechanism: (i) no intermediate can be detected from cyclic voltammetry up to several thousand volts per second corresponding to experimental times in the some tenths of a millisecond; (ii) it was not possible to find another stable conformation more similar to the neutral species with molecular modeling; (iii) flash photolysis experiments show that the final radical cations are already produced for times shorter than 50–100 ns after the pulse [22].

To explain the apparently fast electron transfers observed experimentally and to see if data were in agreement with the concerted mechanism, we estimated the different contributions to the activation barrier for the electron transfer in the framework of the Marcus–Hush model [44–48]. The reorganization free energy of the electron transfer λ_{elec} is divided into a solvent reorganization term, $\lambda_{0,elec}$, and an intramolecular reorganization term, $\lambda_{i,elec}$, $\lambda_{elec} = \lambda_{0,elec} + \lambda_{i,elec}$. For the first electron transfer, the electrochemical reorganization energy can be derived from the experimental electrochemical standard rate constants $k_{s,1}$, uncorrected from the double layer effect: $k_s = Z^{el} \exp[(-F(\lambda_{0,elec} + \lambda_{i,elec}))/(4RT)]$ with $Z^{el} = \sqrt{(RT)/(2\pi M)}$ (M, molar mass) and $\lambda_{0,elec} = (3/a)$ (a, radius of the equivalent sphere in Å) [49]. $\lambda_{i,elec}$ can be estimated from the difference in energy between the neutral TTF at its equilibrium geometry and at the equilibrium geometry of the radical cation and conversely, from the difference in energy between the radical cation at its equilibrium geometry and at the equilibrium geometry of the neutral TTF [50,51]. Experimental $k_{s,1}$ values were estimated from the variation of the peak potentials with the scan rates. The same procedure allows the determination of $\Delta E° = E_2^\circ - E_1^\circ$ taking into account the effects of the electron transfer kinetics. The $\Delta E°$ precisions for **4f** and **5** were good (lower than 5 mV), but for **4b** because of the large potentials inversion, a possible fitting was obtained between 0.1 and 0.15 V (see Ref. [22] for details about the measurements of $k_{s,1}$). Experimental and theoretical values for the activation barriers are given in Table 4.

Even if the experimental $k_{s,1}$ values are approximate, the comparison of the experimental data with theoretical parameters shows a good agreement with the occurrence of an EE mechanism in which the electron transfer is concerted with the conformation changes. However, the inner reorganization energies remain modest (0.35–0.45 eV) allowing a fast passage between different conformations during electron transfer. This last point is particularly interesting for the design of new functional materials.

4. Conclusion

The preparation of substituted vinylogous TTF by oxidative coupling of DTF is a convenient method for introducing different substituents on the central conjugation of the TTF core. After fast electron transfer, the generated cation radicals undergo fast dimerization into a protonated dimer. Then, this protonated dication slowly deprotonates into the expected TTF vinylogue. Through the adjustment of the DTF structure and substituent choice, it is possible to control the relative stabilities of the different redox species of the produced TTF vinylogues. At one end, the structural changes induced by the steric interactions lead to a compression of potentials where the second electron transfer is much easier than the first one. At the other end, opposite

situations are obtained with a large increase of the separation between the first and second oxidation potentials compared to similar molecules without steric hindrance.

References

[1] G. Schukat, E. Fanghänel, Sulfur Rep. 18 (1996) 1.
[2] T. Sugimoto, H. Awaji, I. Sugimoto, Y. Misaki, T. Kamase, S. Yoneda, Z. Yoshida, T. Kobayashi, H. Anzai, Chem. Mater. 1 (1989) 535.
[3] T.K. Hansen, M.V. Lakshmikantham, M.P. Cava, R.M. Metzger, J. Becher, J. Org. Chem. 56 (1991) 2720.
[4] A.J. Moore, M.R. Bryce, D.J. Ando, M.B. Hursthouse, J. Chem. Soc., Chem. Commun. (1991) 320.
[5] A.J. Moore, M.R. Bryce, Tetrahedron Lett. 33 (1992) 1373.
[6] M.R. Bryce, M.A. Coffin, W. Clegg, J. Org. Chem. 57 (1992) 1696.
[7] M.R. Bryce, A.J. Moore, B.K. Tanner, R. Whitehead, W. Clegg, F. Gerson, A. Lamprecht, S. Pfenninger, Chem. Mater. 8 (1996) 1182.
[8] W. Kirmse, L. Horner, Liebigs Ann. Chem. 614 (1958) 4.
[9] M.P. Cava, M.V. Lakshmikantham, J. Heterocycl. Chem. 17 (1980) S39.
[10] U. Schöberl, J. Salbeck, J. Daub, Adv. Mater. 4 (1992) 41.
[11] D. Lorcy, R. Carlier, A. Robert, A. Tallec, P. Le Maguerès, L. Ouahab, J. Org. Chem. 60 (1995) 2443.
[12] P. Hapiot, D. Lorcy, R. Carlier, A. Tallec, A. Robert, J. Phys. Chem. 100 (1996) 14823.
[13] H. Hopf, M. Kreutzer, P.G. Jones, Angew. Chem., Int. Ed. Engl. 30 (1991) 1127
[14] A. Benahmed-Gasmi, P. Frère, J. Roncali, E. Elandaloussi, J. Orduna, J. Garin, M. Jubault, A. Gorgues, Tetrahedron Lett. 36 (1995) 2983.
[15] N. Bellec, D. Lorcy, A. Robert, R. Carlier, A. Tallec, J. Electroanal. Chem. 462 (1999) 137.
[16] A. Ohta, Y. Yamashita, J. Chem. Soc., Chem. Commun. (1995) 1761.
[17] Y. Yamashita, M. Tomura, M. Braduz Zaman, K. Imaeda, J. Chem. Soc., Chem. Commun. (1998) 1657.
[18] A.J. Moore, M.R. Bryce, P.J. Skabara, A.S. Batsanov, L.M. Goldenberg, J.A.K. Howard, J. Chem. Soc., Perkin Trans. 1 (1997) 3443.
[19] P. Hascoat, D. Lorcy, A. Robert, R. Carlier, A. Tallec, K. Boubekeur, P. Batail, J. Org. Chem. 62 (1997) 6086.
[20] M. Fourmigué, I. Johannsen, K. Boubekeur, C. Nelson, P. Batail, J. Am. Chem. Soc. 115 (1993) 3752.
[21] S. Gonzalez, N. Martin, L. Sanchez, J.L. Segura, C. Seoane, I. Fonseca, F.H. Cano, J. Sedo, J. Vidal-Gancedo, C. Rovira, J. Org. Chem. 64 (1999) 3498.
[22] N. Bellec, K. Boubekeur, R. Carlier, P. Hapiot, D. Lorcy, A. Tallec, J. Phys. Chem. A 104 (2000) 9750.
[23] D.H. Evans, K.M. O'Connell, in: A.J. Bard (Ed.), Conformational Change and Isomerization Associated with Electrode Reactions in Electroanalytical Chemistry, vol. 14, Marcel Dekker, New York, 1986, pp. 113–207.
[24] D.H. Evans, M.W. Lehmann, Acta Chem. Scand. 53 (1999) 765.
[25] D.H. Evans, K. Hu, J. Chem. Soc., Faraday Trans. 92 (1996) 3983.
[26] K. Hu, D.H. Evans, J. Phys. Chem. 100 (1996) 3030.
[27] K. Hu, D.H. Evans, J. Electroanal. Chem. 423 (1997) 29.
[28] B. Speiser, M. Würde, C. Maichle-Mössmer, Chem. Eur. J. 4 (1998) 222.
[29] S. Dümmling, B. Speiser, N. Kuhn, Weyers Acta Chem. Scand. 53 (1999) 876.
[30] K. Akiba, K. Ishikawa, N. Inamoto, Bull. Chem. Soc. Jpn. 51 (1978) 2674.
[31] D. Garreau, J.-M. Savéant, J. Electroanal. Chem. 35 (1972) 309.
[32] C.P. Andrieux, D. Garreau, P. Hapiot, J. Pinson, J.-M. Savéant, J. Electroanal. Chem. 243 (1988) 321.
[33] M. Rudolph, D.P. Reddy, S.W. Felberg, Anal. Chem. 66 (1994) 589A.
[34] M.J. Frisch, G.W. Trucks, H.B. Schlegel, G.E. Scuseria, M.A. Robb, J.R. Cheeseman, V.G. Zakrzewski, J.A. Montgomery, R.E. Stratmann, J.C. Burant, S. Dapprich, J.M. Millam, A.D. Daniels, K.N. Kudin, M.C. Strain, O. Farkas, J. Tomasi, V. Barone, M. Cossi, R. Cammi, B. Mennucci, C. Pomelli, C. Adamo, S. Clifford, J. Ochterski, G.A. Petersson, P.Y. Ayala, Q. Cui, K. Morokuma, D.K. Malick, A.D. Rabuck, K. Raghavachari, J.B. Foresman, J. Cioslowski, J.V. Ortiz, B.B. Stefanov, G. Liu, A. Liashenko, P. Piskorz, I. Komaromi, R. Gomperts, R.L. Martin, D.J. Fox, T. Keith, M.A. Al-Laham, C.Y. Peng, A. Nanayakkara, C. Gonzalez, M. Challacombe, P.M.W. Gill, B.G. Johnson, W. Chen, M.W. Wong, J.L. Andres, M. Head-Gordon, E.S. Replogle, J.A. Pople, GAUSSIAN 98 (Revision A.1), Gaussian Inc., Pittsburgh, PA, 1998.
[35] C.P. Andrieux, L. Nadjo, J.-M. Savéant, J. Electroanal. Chem. 42 (1973) 223.
[36] C.P. Andrieux, J.-M. Savéant, in: C.F. Bernasconi (Ed.), Investigation of Rates and Mechanism of Reactions, Part 2, vol. 6 4/E, Wiley, New York, 1986, pp. 305–390.
[37] R.L. Myers, I. Shain, Anal. Chem. 41 (1969) 980.
[38] C.P. Andrieux, J.-M. Savéant, J. Electroanal. Chem. 57 (1974) 27.
[39] D. Lorcy, P. Le Maguerès, C. Rimbaud, L. Ouahab, P. Delhaes, R. Carlier, A. Tallec, A. Robert, Synth. Met. 86 (1997) 1831.
[40] C. Rimbaud, P. Le Maguerès, L. Ouahab, D. Lorcy, A. Robert, Acta Crystallogr. C 54 (1998) 679.
[41] A.D. Becke, J. Chem. Phys. 98 (1993) 5648.
[42] P.C. Hariharan, J.A. Pople, Chem. Phys. Lett. 16 (1972) 217.
[43] J.B. Foresman, T.A. Keith, K.B. Wiberg, J. Snoonian, M.J. Frisch, J. Phys. Chem. 100 (1996) 16098.
[44] R.A. Marcus, J. Chem. Phys. 24 (1956) 966.
[45] R.A. Marcus, J. Chem. Phys. 24 (1956) 979.
[46] N.S. Hush, J. Chem. Phys. 28 (1958) 962.
[47] N.S. Hush, Trans. Faraday Soc. 57 (1961) 557.
[48] R.A. Marcus, J. Chem. Phys. 43 (1965) 679.
[49] C.P. Andrieux, J.-M. Savéant, C. Tardy, J. Am. Chem. Soc. 120 (1998) 4167.
[50] A. Klimkans, S. Larsson, Chem. Phys. 189 (1994) 25.
[51] B. Brielbeck, J.C. Rühl, D.H. Evans, J. Am. Chem. Soc. 115 (1993) 11898.